139

SENSITIVITY OF SIMULATED CONVECTIVELY COUPLED KELVIN WAVES TO CUMULUS SCHEMES AND RESOLUTION WITH AN IDEALIZED TROPICAL CHANNEL

Joaquin E. Blanco*[1], David S. Nolan[1] and Stefan N. Tulich[2]

1 Rosenstiel School of Marine and Atmospheric Science, University of Miami, Miami, FL
2 CIRES/University of Colorado and NOAA/ESRL, Boulder, CO

1. INTRODUCTION

Zonally propagating convective activity represents a significant component of the total variability along the intertropical convergence zone (ITCZ). Westward propagating convective clusters along the Equator coexist with eastward propagating cumulus activity, organized in a hierarchy of time and spatial scales. Convectively Coupled Kelvin Waves (CCKWs) are envelopes of enhanced convection that propagate eastward in a range of velocities that is typically between 12-18m/s. The coherent structure of the CCKW can remain distinguishable over weeks, and it can be often tracked all the way around the globe. The individual cells within the CCKWs propagate westward with slower speeds and a lifetime of 1-2 days.

The CCKWs are the moist counterparts of the dry Kelvin Waves, which propagate twice as fast, have no meridional velocity, are non-dispersive and can be understood as gravity waves in the east-west direction with geostrophic balance between zonal wind and meridional pressure gradient (Matsuno 1966). The CCKWs were originally referred to as Super Cloud Clusters or Superclusters because of the aforementioned characteristics, which are clearly identifiable in satellite imagery (Nakazawa 1988; Takayabu and Murakami 1991; Takayabu 1994). Some of these early works focused mainly on case studies, but when reanalysis became available, composites of different variables were produced to investigate the structure and dynamics of these waves. Simultaneously, evidence of Superclusters appeared in idealized aquaplanet simulations (Hayashi and Sumi 1986; Hayashi and Nakazawa 1989) conducted for investigation of the Madden-Julian oscillation (MJO).

More recently, the entire spectrum of Convectively Coupled Equatorial Waves (CCEWs) has become a vast subject of study (involving both observed and simulated cases), with special emphasis on their multiple interactions as well as the amount of variance explained by a particular wave over the total. In particular, a widely used technique consists in a filtering of the data in the frequency-wavenumber space within a power spectrum, to isolate the different CCEWs (Wheeler and Kiladis 1999; Straub and Kiladis 2002; Straub and Kiladis 2003; Roundy and Frank 2004; Roundy 2008).

The present work studies structure and propagation speeds of idealized CCKWs using the ARW-WRF model, with a sensitivity analysis to cumulus schemes and horizontal resolution. Next section describes the model set-up and schemes used for the experiments. The methodology for tracking the CCKWs is presented in section 3. The propagation speeds and spatial structures of the waves are shown and analyzed in sections 4.A and 4.B, respectively, followed by summary and conclusions (section 5).

2. MODEL AND SIMULATIONS

The simulations are performed in an equatorial β-channel with no topography, and 40km resolution over a domain 13200km x 13200km in size (330x330 points). The grid extends from 60ºS to 60ºN (free-slip walls) and has periodic boundary conditions in the zonal direction. Vertical spacing is variable in the range of 100-450m, with model top at about 28km (level 64).

The forcing of the model is a prescribed symmetric SST profile (see Fig. 1), and spin-up time is 1 year. The Goddard scheme is used for both SW and LW radiation and the Goddard GCE scheme for cloud microphysics. Four experiments are performed using the Betts-Miller-Janjic (BM) and Kain-Fritsch (KF) cumulus schemes and the activation (or not) of a 2-way nested channel in a tropical belt (+/- 16º) with 8km spacing, where convection is solved explicitly.

Precipitation along the ITCZ is very sensitive to the cumulus scheme; the time-zonal mean of precipitation for the 4 experiments is shown in Fig. 2. The BM simulation shows a sharp ITCZ centered on the equator, while for the KF case it is asymmetric, double-peaked and weaker. When convection is solved explicitly in the tropical channel (NC cases), less precipitation is produced in comparison with the no-nesting counterparts.

* Corresponding author address: Joaquin Esteban Blanco. University of Miami / RSMAS, 4600 Rickenbacker Causeway, Miami, FL, 33149-1098. email: jblanco@rsmas.miami.edu

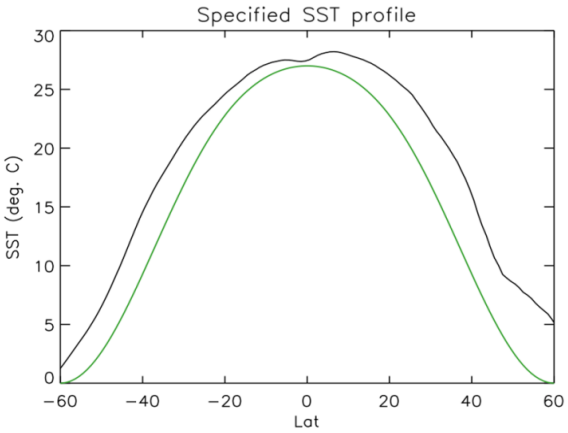

Figure 1: “observed” SST profile from the aquaplanet intercomparison project of Neale and Hoskins (2000) used for the simulations (green), and observed zonal mean SST profile (black).

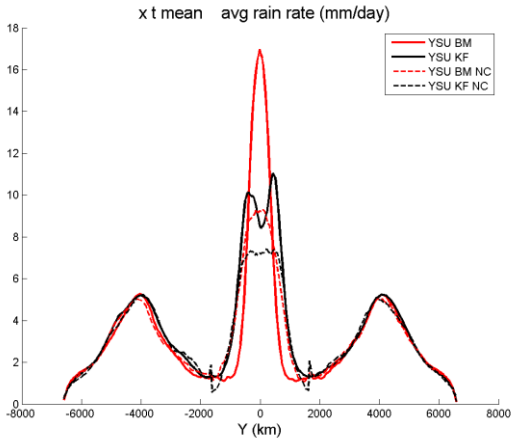

Figure 2: “Model climatology” for the 4 simulations.

3. METHODOLOGY

An algorithm was applied to track the CCKW propagation along the equator. Several variables were tested for wave tracking: maximum rain rates, minimum OLR, maximum total q_v at 500hPa, minimum divergence at 850hPa, minimum zonal wind at 200hpa, and maximum surface pressure.

Fig. 3 shows an example of the tracking of a CCKW over a 5-day period, using precipitation or surface pressure. The maximum/minimum is tracked in a narrow tropical band (+/-600 km or +/-15 grid points from the equator), and smoothing was applied to the field to reduce noise. In particular, smoothing was essential when precipitation was used, in order to track the “envelope” of convection rather than picking the strongest individual cell in the tropics at every time step. However, the CCKW axis had no “stable” propagation because of the individual cells propagating westward within the CCKW moving in a wide range of speeds from -5 (westward) grid points per time step to about +20 (eastward), and therefore, an additional constraint of minimum and maximum phase speed of 1 to 15 grid points per time step (1.85 to 27.77 m/s) was imposed. Because of this constraint on the phase speed of the CCKW, its axis might not coincide with the actual maximum or minimum of the variable at a given time step (shown in Fig. 3). After several tests, precipitation was discarded as a tracker and maximum of surface pressure was chosen. It is important to note that the maximum surface pressure usually lags behind the most active convection by about 500-1000km. Hereafter the CCKW axis will be identified by the maximum surface pressure (p_{surf}).

Fig. 4 shows for the BM simulation a time-longitude plot indicating the position and velocity at which the CCKW axis propagates eastward at every time step, during a period of 75 days. The algorithm applies an update every 10 time steps in which the maximum value of p_{surf} is searched again in the entire length of the 600km-width channel, rather than 1-15 grid point band ahead of the wave axis. This was introduced in order to prevent the tracking of a hypothetically weakening CCKW at the time a stronger wave signal appears in another region of the domain. This is evidenced in Fig. 4 with the discontinued line; however, many of these “jumps” of the CCKW axis are due to faster wave propagation at the time of the update (i.e. exceeding a 15 grid point displacement in that time step).

Composites for different variables are calculated following the CCKW as it propagates eastward. With reference to the maximum surface pressure p_{surf} all 2D and 3D variables are shifted in the east-west direction and averaged in time (model outputs are in 6-hour intervals). The axis of the composited CCKW is relocated to the center of the domain. Composites for some variables and comparisons among the experiments are analyzed in section 4.B.

4. RESULTS

4.A. Phase Speeds

The mean CCKW phase speed for the BM and BM NC experiments are 17.0m/s and 16.3m/s respectively, while for the KF and KF NC experiments they are 13.0m/s and 14.5m/s.

In order to understand the differences among the 4 simulations, the background state was analyzed. A time and zonal mean was applied to static stability and zonal wind, and then an average between 5ºS and 5ºN was taken to study the mean vertical structure along in the tropics (Fig. 5). While for static stability all simulations show similar vertical structure, striking differences appear for the zonal wind at certain levels. Stronger currents for the BM simulations between 8 and 13 km height might explain the faster propagation of their CCKWs.

However, the BM case has the higher *Cx* value (17.0m/s) while the stronger *u* at high levels corresponds to the BM NC case; more is yet to be analyzed before concluding on the causes of these differences.

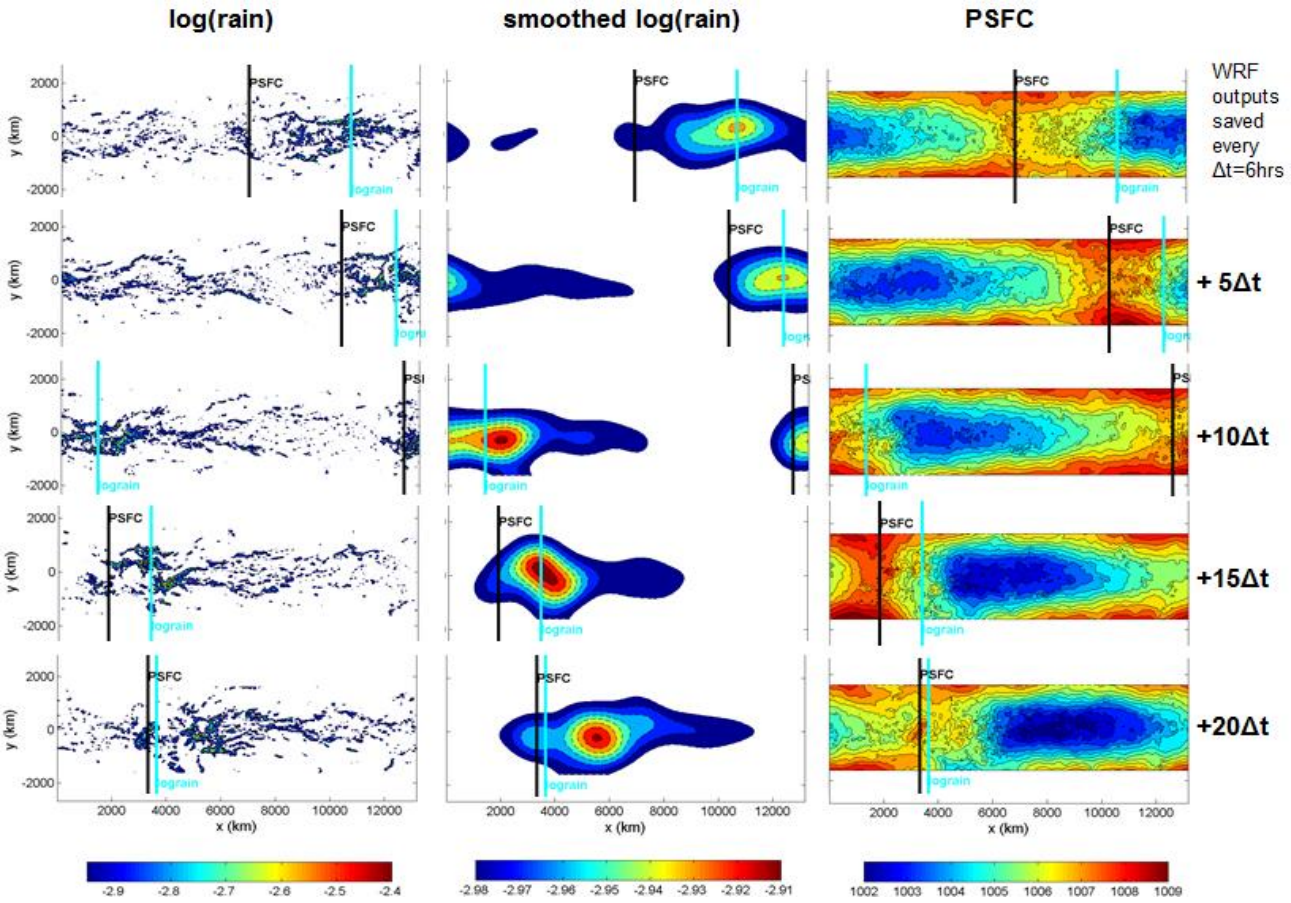

Figure 3: Sequence every 30 hours of average rain rate (raw field on left, smoothed 550 times in the center) and surface pressure (smoothed 50 times, on right). These smoothed fields were used at every time step for finding the maximum/minimum of the variable, of which the x-location is indicated for both variables.

4.B. Composites

The zonal mean of the composite (time and zonal mean of the raw variable) is subtracted to obtain the perturbation composite. For all cases, the overall findings are as follows:

Along the equator, elongated regions of negative (positive) anomalies of OLR (precipitation) extend from about 500 km west of the CCKW axis up to 2000-4000km to the east, while anomalies with the opposite sign extends to the rest of the domain (Fig. 6). The minimum OLR anomalies are at the center of the domain (i.e.: collocated with the maximum pressure anomalies). At low levels, westerlies in the equator are collocated with the CCKW, with convergence ahead of its axis and divergence behind (Fig. 6). At high levels, the reverse is found: easterlies, divergence ahead and convergence behind, with well-defined anticyclonic cells in both hemispheres (Fig. 6). A 10-grid point meridional mean of vertical cross sections centered

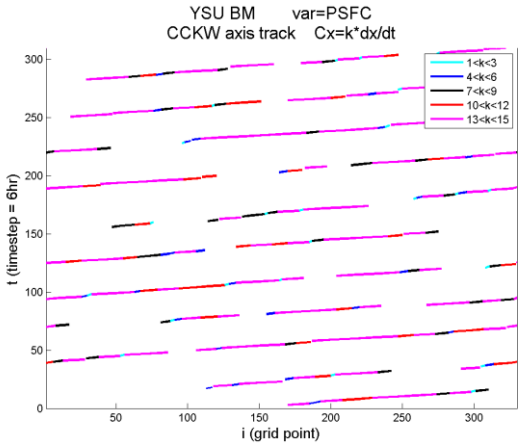

Figure 4: Eastward propagation of the CCKW axis for the BM case. At every time step a new location of the CCKW is estimated (see details in text). 1 Δx/Δt = 1.8519 m/s.

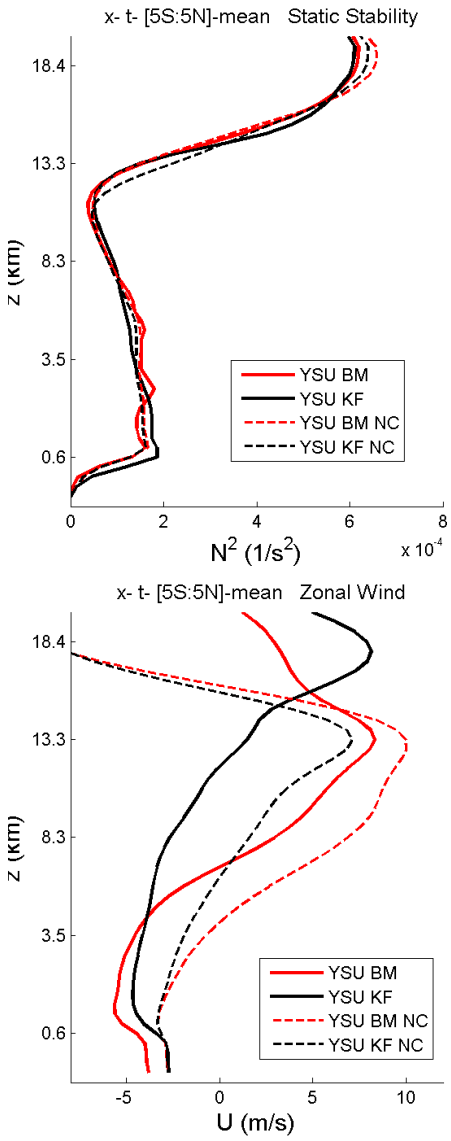

Figure 5: Vertical structure of static stability and zonal wind (time and zonal mean, 10º mean around the equator) for the 4 simulations.

at the equator indicates deep structures with westward phase tilt with height for moist static energy (not shown), divergence (not shown) and vertical wind (Fig. 6), and a boomerang-like shape for the zonal wind field (i.e.: westward tilt in the lower half of the domain, eastward tilt in the upper half). This last feature is shown in Fig. 7 for the 4 cases. In most of the analyzed perturbation composites, the signal is much weaker for the KF experiment (with smaller propagation speed), and among the other 3 simulations, the KF NC is weaker but the difference is not too significant (see Figs. 7 and 8).

A striking feature was observed in the total cloud condensate (precipitating + nonprecipitating) for the KF case: most of the convection in concentrated in a shallow layer right above the top of the boundary

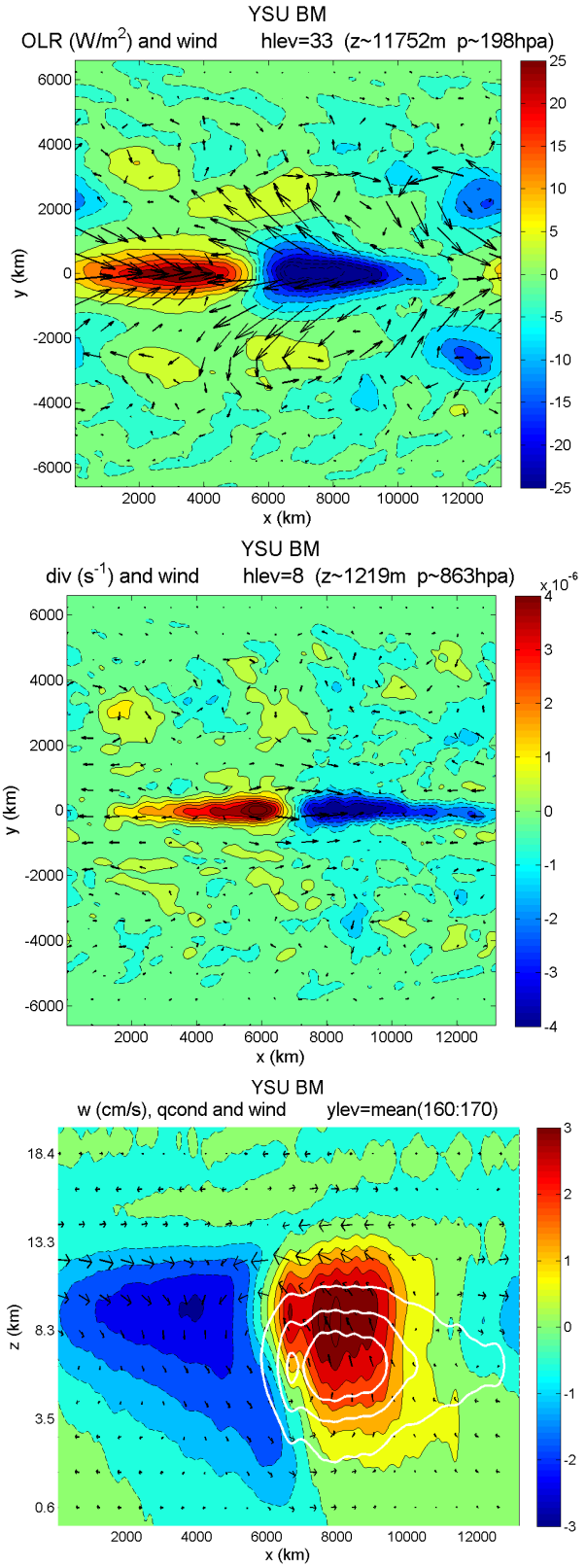

Figure 6: composites for the BM simulation. Top: OLR (shaded) and wind (vectors) at ~200hpa; center: divergence (shaded) and wind (vectors) at ~850hpa; bottom: vertical wind (shaded), vertical-zonal wind (vectors), and total composite (not perturbation) of cloud condensate (heavy white contours).

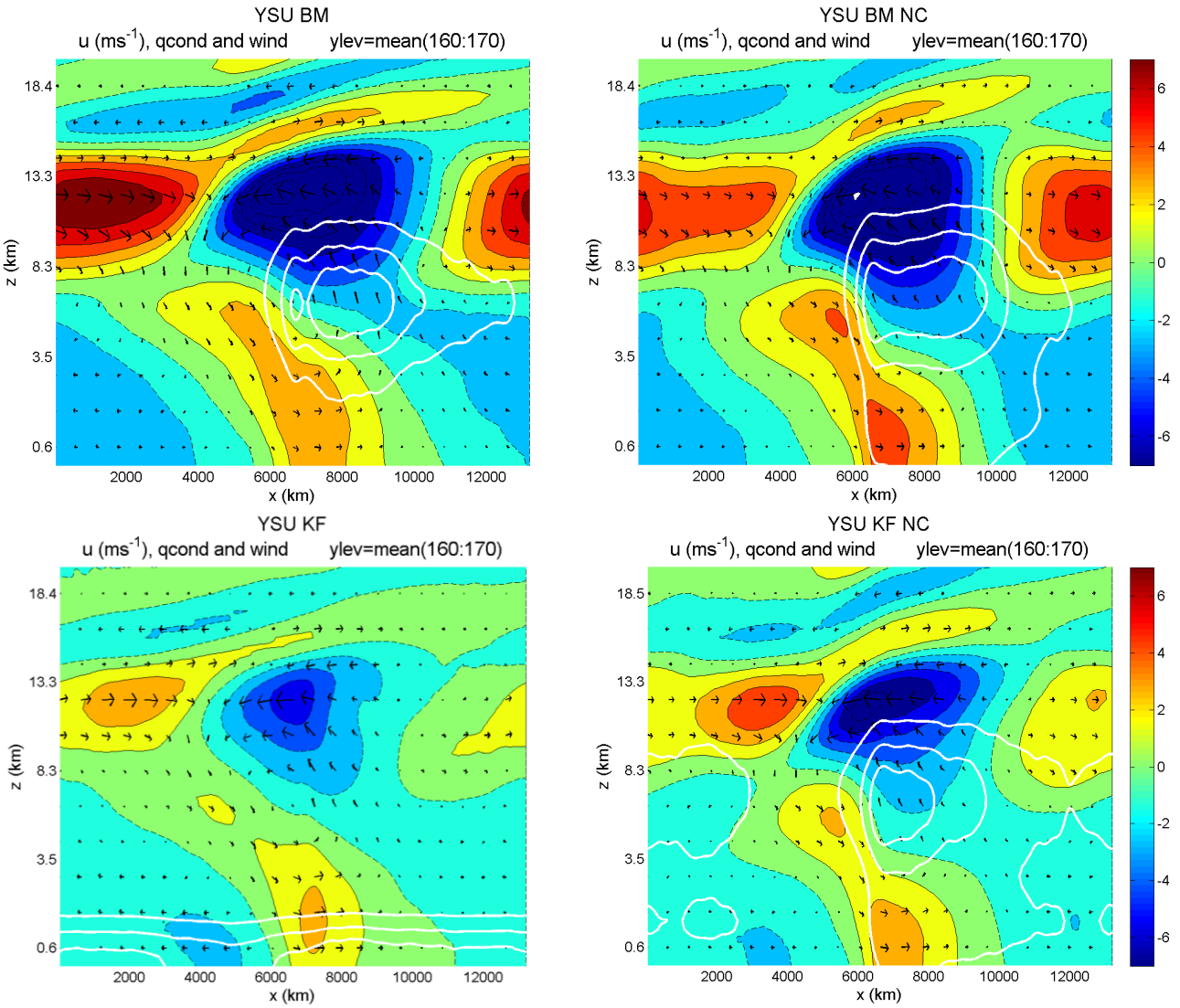

Figure 7: Perturbation composite of zonal wind (shaded) and vertical-zonal wind (vectors) and total composite (not perturbation) of cloud condensate (heavy white contours), for the 4 simulations.

layer (shown in the KF panel in Fig. 7). This anomaly appears to be due to an unrealistic representation of convection by the KF scheme.

Since maximum rain rates were not used as the tracking variable, the composites for the 4 simulations are shown in Fig. 8: a zonally-broader region of precipitation is present in the BM and BM NC cases, which in turn is stronger than in the KF counterparts. Also, the BM signal is also more confined to the equator, where the other 3 cases it extends more meridionally.

Finally, despite using the same model configuration in the tropics for both BM NC and KF NC simulations, significant differences appear in the tropics, which are due to extratropical interactions.

5. CONCLUDING REMARKS

This study analyzed the sensitivity of CCKWs to cumulus parameterization and resolution in an "aquapatch" with the WRF-ARW model. Four experiments were conducted, using the Betts-Miller-Janjic or Kain-Fritsch scheme, combined with the activation or not of a high-resolution nested channel in the tropics where convection is solved explicitly.

No filtering in the frequency-wavenumber space was applied, and therefore an algorithm with special conditions was designed for tracking CCKWs. The focus of this work was on the phase speed of the waves as well as on its structure, and for the latter purpose composites of different variables were analyzed.

We found that propagation speeds of the CCKW are in the range of 13-17 m/s, and these differences might be attributed to differences in the zonal flow in the tropics.

Overall, the dynamic fields associated to the CCKW are as follows. At low levels, westerlies, convergence ahead and divergence behind the wave axis, whereas at high levels the opposite holds

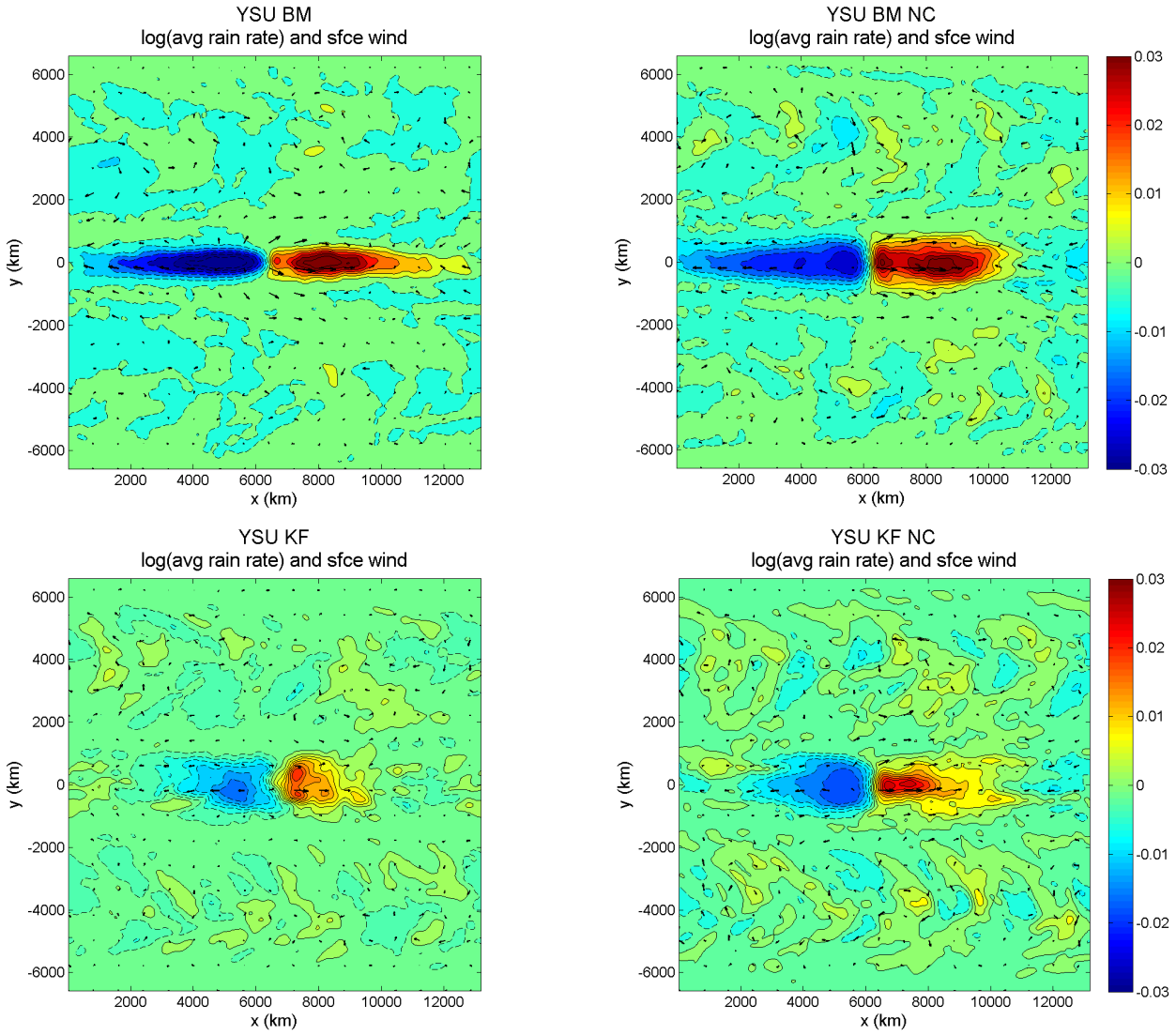

Figure 8: Perturbation composite of logarithm of precipitation rates (shaded) and surface wind (vectors), for the 4 simulations.

(i.e: easterlies, divergence ahead and convergence behind) but with stronger magnitudes and with well-defined anticyclonic cells in both hemispheres. Vertical cross sections at the equator indicate deep structures, westward phase tilt with height and a boomerang-like shape for zonal wind. It is important to point out that these patterns are in agreement with previous studies (Nakazawa 1988; Straub and Kiladis 2002), regardless of the use or not of a filtering technique to isolate the CCKW, the algorithm for tracking it, and the nature of the data (e.g., reanalysis, real-data simulations, or idealized simulations). The composited structure of the CCKWs is similar to those of the MJO.

More analysis remains pending for better understanding of the different wave speeds and structures of the CCKWs in terms of their dynamics among the 4 experiments. Finally, the filtering technique approach will be applied to the data and the new composites will be compared to the ones found for this study.

Acknowledgements. This research was supported by the National Science Foundation grant AGS-1146701.

REFERENCES

Hayashi Y.-Y. and T. Nakazawa,1989: Evidence of the Existence and Eastward Motion of Superclusters at the Equator. *Mon. Wea. Rev.*, **117**, 236-243.

Hayashi Y.-Y. and A. Sumi,1986: The 30-40 day oscillations simulated in an “aqua-planet” model. *J. Meteorol. Soc. Jpn.*, **64**, 451-467.

Matsuno, T., 1966: Quasi-geostrophic motions in the equatorial area. *J. Meteor. Soc. Japan*, **44**, 25-43.

Nakazawa, T., 1988: Tropical super clusters within Intraseasonal Variations over the Western Pacific. *J. Meteorol. Soc. Jpn.*, **66**, 823-839.

Roundy, P. E., 2008: Analysis of Convectively Coupled Kelvin Waves in the Indian Ocean MJO. *J. Atmos. Sci.*, **65**, 1342–1359.

Roundy, P. E., and W. M. Frank, 2004: A climatology of waves in the equatorial region. *J. Atmos. Sci.*, **61**, 2105–2132.

Straub, K. H., and G. N. Kiladis, 2002: Observations of a convectively coupled Kelvin wave in the eastern Pacific ITCZ. *J. Atmos. Sci.*, **59**, 30–53.

Straub, K. H., and G. N. Kiladis, 2003: The observed structure of convectively coupled Kelvin waves: Comparison with simple models of coupled wave instability. *J. Atmos. Sci.*, **60**, 1655–1668.

Takayabu, Y. N., 1994: Large-scale cloud disturbances associated with equatorial waves. Part I: Spectral features of the cloud disturbances. *J. Meteor. Soc. Japan*, **72**, 433–448.

Takayabu, Y. N., and M. Murakami, 1991: The structure of super cloud clusters observed in 1–20 June 1986 and their relationship to easterly waves. *J. Meteor. Soc. Japan*, **69**, 105–125.

Wheeler, M. and G. N. Kiladis, 1999: Convectively coupled equatorial waves: Analysis of cloud and temperature in the wavenumber-frequency domain. *J. Atmos. Sci.*, **56**, 374-399.